Decoherence-Free Rotational Degrees of Freedom for Quantum Applications

J. S. Pedernales, F. Cosco, and M. B. Plenio
Institut für Theoretische Physik und IQST, Albert-Einstein-Allee 11, Universität Ulm, D-89081 Ulm, Germany

(Received 14 January 2020; accepted 21 July 2020; published 26 August 2020)

We employ spherical t-designs for the systematic construction of solids whose rotational degrees of freedom can be made robust to decoherence due to external fluctuating fields while simultaneously retaining their sensitivity to signals of interest. Specifically, the ratio of signal phase accumulation rate from a nearby source to the decoherence rate caused by fluctuating fields from more distant sources can be incremented to any desired level by using increasingly complex shapes. This allows for the generation of long-lived macroscopic quantum superpositions of rotational degrees of freedom and the robust generation of entanglement between two or more such solids with applications in robust quantum sensing and precision metrology as well as quantum registers.

DOI: 10.1103/PhysRevLett.125.090501

Introduction.—Quantum metrology and sensing represent promising near term applications of quantum technologies as they require the control of a few or even single quantum systems. A wide variety of physical systems are being developed for these purposes ranging from solid state spins [1] to ultracold trapped atoms and ions [2], atom interferometry [3], optomechanical systems [4], and levitated massive particles [5].

A central challenge common to all quantum sensor designs is the necessity to achieve both robustness to environmental noise and, at the same time, high sensitivity to a signal of interest. To this end, while affecting the signal as little as possible, we need to either filter noise, correct for its effect, or encode the system to reduce its sensitivity to environmental noise. This becomes possible whenever signal and noise have some characteristic in which they differ. Frequently used examples include cases in which signal and noise differ in spectral or temporal support, in the symmetries of signal and noise or in the operator with which they act on the system. These allow us to separate signal and noise, e.g., via dynamical decoupling [6–12], time gating, decoherence-free subspaces [13,14], or quantum error correction [15–20], respectively.

The principles of levitation and feedback cooling of massive particles in a high vacuum have been demonstrated by Ashkin [21,22] and with it came the recognition that such systems are promising for ultraprecise metrology and sensing due to the lack of friction and a high degree of isolation from nearby sources of noise and decoherence. Reference [5] was the first to propose their use in the quantum regime and this has led to theoretical and experimental work towards the cooling of optically levitated silica nanomicrospheres [23–29], magnetically levitated diamond [30], and silica nanocrystals [31]. The control of single electron spins in trapped diamond nanocrystals was first demonstrated in [32–34] motivating subsequent theoretical explorations [35–37] as well as further experimental works that include the control of their torsional degrees of freedom under optical forces [38] and ion traps [39,40]. An important long term goal in this field is the realisation of tests for possible minute deviations from quantum physics [35–37,41–43], for the detection of corrections of known force laws due to extra dimensions [44] and new forces and particles [45,46] or the realization of early proposals of gravitationally induced entanglement [47,48] using levitated particles [49–53]. A common goal of many of these approaches is the detection of minute interactions with nearby sources in the presence of noise from more distant sources. However, current proposals for matter-wave interferometry with translational degrees of freedom of massive particles are susceptible to first order (gradient) fluctuations and hence perturbing signals of the same nature emanating even from distant sources [54]. Therefore, we are faced with the challenge of suppressing perturbations from distant sources without suppressing the desired signals from nearby sources.

In this Letter, we address this challenge by designing the shape of rigid bodies such that their *rotational* degrees of freedom can be made robust against decoherence from distant sources, while at the same time allowing for interaction with signals from nearby sources. To this end we introduce a systematic method, based on the mathematical theory of spherical t-designs, to construct rigid bodies whose rotational states are degenerate up to a desired order of the multipole expansion of their energy in a perturbing potential. In this manner, we ensure that superpositions in the basis of rotational states of a suitably designed solid can, in principle, exhibit arbitrarily long coherence times in the presence of perturbations from distant sources. Moreover, we show that the ratio of the entangling to decoherence rate between two of these objects scales favorably with the order of the spherical t-design.

Multipole expansion and spherical t-designs.—Consider a rigid body that is held in free space and whose rotational degrees of freedom we aim to control and place in superposition of different orientations of this body. The elimination of decoherence of such a superposition requires the construction of an object whose potential energy in an external field is the same for all of its orientations, so that when the object is placed in a superposition of two different orientations, fluctuations of the perturbing field translate into global phase variations, keeping the relative phase of the superposition constant, and in this manner preserving its coherence. A shape which, thanks to its rotational symmetry, trivially fulfils such a goal is that of a uniform sphere. However, it is important to note that such an object is, for our purposes, useless as the different orientations of a sphere are indistinguishable, and, as a consequence, superpositions of different orientations of the sphere become experimentally inaccessible. Therefore, our goal will be the design of a body that decouples from the external fields as well as possible and, simultaneously, deviates as much as possible from the spherical symmetry, such that different orientations of such a body can be placed in superposition and can be made to interact between two such bodies.

For a system whose center of mass is placed at the origin of coordinates, the perturbing field generated by a distant source admits a multipole expansion $\phi(\vec{x}) = \sum_{n=0}^{\infty}\sum_{i_1,\ldots,i_n=1}^{3} M_{i_1,\ldots,i_n}(\vec{x})_{i_1}\cdot,\ldots,\cdot(\vec{x})_{i_n}$, where $M_{i_1,\ldots,i_n}$ are the nth order moments of the field. The nth order moments will scale as $1/L^n$, where L is the distance to the object generating the perturbing field. The total energy of an object with a density distribution $\rho(\vec{x})$ in such a potential is given by $V = \int d\vec{x}\rho(\vec{x})\phi(\vec{x})$. Hence, for perturbing fields that originate at distances much bigger than the spatial extent R of the body, the contribution of the nth order moment to the energy will scale as $(R/L)^n$ and consequently become rapidly negligible.

In order to reduce decoherence from distant fields, we will engineer a density distribution that results in rotationally invariant contributions to V up to a given order of the multipole expansion so that only higher moments can contribute to decoherence. For simplicity, we construct our distribution as $\rho(\vec{x}) = q\sum_{i=1}^{N}\delta(\vec{x}-\vec{P}_i)$, that is, a collection of a finite number N of point charges and masses q located at positions $\vec{P}_i$. A systematic strategy to achieve this makes use of the concept of spherical t-designs [55,56] which is a set of N points $\{\vec{P}_i\}$ on the unit sphere of dimension $d+1$, $S^d = \{\vec{x}\in\mathbb{R}^{d+1}:\vec{x}\cdot\vec{x}=1\}$, which satisfies

$$\int_{S^d} f(\vec{x})d\mu(\vec{x}) = \frac{1}{N}\sum_{i=1}^{N} f(\vec{P}_i), \qquad (1)$$

for all polynomials of degree less or equal to t, $f(\vec{x}) = \sum_{n=1}^{t}\sum_{i_1,\ldots,i_n=1}^{3} c_{i_1,\ldots,i_n}(\vec{x})_{i_1},\ldots,(\vec{x})_{i_n}$.

Equation (1) implies that, for such a density, the contributions to the total energy are invariant under rigid rotations up to order t in the multipole expansion. This follows from the linearity of the rotation operation in terms of coordinate variables, which guarantees that the potential function truncated at order t transforms into a polynomial of the same order in a rotated frame. Therefore, up to order t, the potential energy of the spherical t-design in the rotated field equals that of a uniform sphere and, as the potential energy of the sphere is evidently invariant under rotations, so is the energy of the t-design up to order t. Now, to relate this result to our aim of designing a solid with a continuous density distribution whose potential energy is invariant under rotations up to order t in the multipole expansion, we note that, for three spatial dimensions, any choice of points on the unit sphere can be extended to a simply connected solid by considering the set of points on all spheres of all radii $r \le 1$ and adopting a finite volume when allowed to trace out a solid angle. For an object constructed in such a manner from a spherical t-design, all contributions up to order t in the multipole expansion of the potential energy are rotationally invariant. A fluctuating external potential field will induce variations in the relative phase between two orientations of such an object only in the $(t+1)$th order of the multipole expansion, whose magnitude decreases exponentially with t, leading to a strong reduction in the decoherence of its rotational degrees of freedom.

The existence of spherical t-designs for any choice of t is well established. In fact, it has been proven that, for each $N \ge c_d t^d$, there exists a spherical t-design in the sphere S^d consisting of N points, where c_d is a constant depending only on d [57] and, most relevant for our work, it is conjectured that $c_2 = 1/2$. For orders $t = \{1,2,3,4,5,7,9\}$, analytic solutions are known with a number of points N that is close to the optimal number of elements [58], while close to optimal numerical solutions have been found up to orders exceeding $t = 300$ [59].

In Fig. 1(b), we plot known analytic solutions that are conjectured to be optimal in N and leave out cases where solutions are only numerical. We show for each of these designs the magnitude of the potential energy contribution due to the first moment of the perturbing potential that is not rotational invariant, demonstrating an exponential decay $(R/L)^{t+1}$; this indicates the magnitude of the fluctuations of the relative phase between any two orientations of that object in a perturbing field.

Our approach displays some resemblance with [60] where coherent superpositions of rotational molecular states are used to enable active quantum error correction using measurement and feedback to achieve protection against angular momentum errors. In contrast our approach achieves this robustness by classically "baking" the robustness into the structure of the rigid body thus avoiding the need for active error correction.

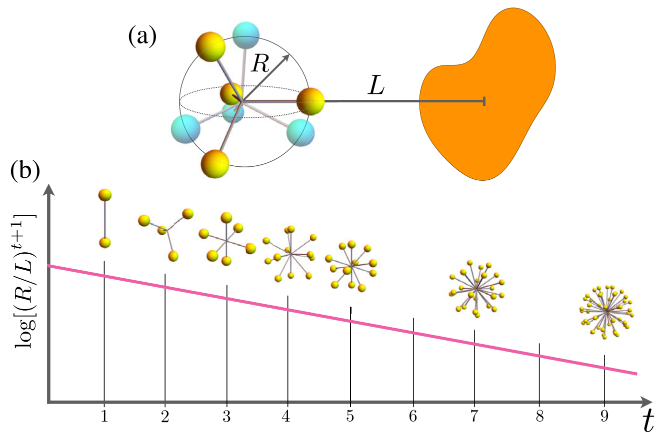

FIG. 1. t-designs in three-dimensional space. Panel (a) depicts a spherical 2-design consisting of points on a sphere of radius R, susceptible to the potential field generated by a distant density distribution (orange object) located at a distance L. Two distinct orientations (blue and yellow) of such a spherical t-design may have different potential energy, however, this difference will originate from moments of the order of 3 and higher in the multipole expansion of the potential field about the center of mass of the body. Panel (b) shows analytical solutions of spherical t-designs up to the order of 9 and the scaling of the energy variations that rotations can induce. The leading order in the potential energy difference between two orientations of a t-design in the field generated by a distant object is provided by moments of order $t+1$, which for the case of a Coulombian potential, scale following the power law $(R/L)^{t+1}$.

Applications.—Objects as described in the previous section may be constructed from nanoparticles and trapped either in optical [61,62], Paul [63], or magnetogravitational traps [30]. The rotational degrees of freedom of irregularly shaped nanoparticles have been manipulated in such settings making use of the torque exerted by circularly polarized light or by magnetic field gradients acting on spin degrees of freedom that the nanoparticles may host, e.g., NV centers in diamond [39,40]. In matter-wave interferometry with translational degrees of freedom of nanoparticles, superpositions are susceptible to first order (gradient) fluctuations of the perturbing fields which, in conjunction with the required long experimental times, set daunting demands on the degree of isolation of the experimental setups [54]. Hence, we propose the use of rotational degrees of freedom of bodies constructed according to spherical t-designs which, due to their extended coherence, are expected to result in a superior performance. For example, a superposition of two orientations of such a nanoparticle would constitute a macroscopic quantum superposition whose lifetime can be used to set bounds on free parameters of continuous spontaneous localization models [64,65].

Furthermore, we stress that the enhancement in the isolation of the rotational degrees freedom of t-designed objects from distant perturbation sources does not prevent them from retaining sensitivity to fields generated by closer sources and thus allows for their application as robust quantum sensors. Consider a t-designed object that is a distance L from a perturbing source and a distance D from the signal source of interest, such that $L/D \gg 1$. When initially prepared in a superposition of two orientations $|R1\rangle + |R2\rangle$, this state will acquire a relative phase at a rate $\bar{\Delta} = \Delta(R1) - \Delta(R2)$ due to the action of signal and perturbing field. As the leading order contributions to this rate due to signal and perturbation, $\bar{\Delta} = \bar{\Delta}_{\text{signal}} + \bar{\Delta}_{\text{noise}}$, originate from the $(t+1)$st order contribution in their multipole expansion, they scale as $\bar{\Delta}_{\text{signal}} \sim (R/D)^{t+1}$ and $\bar{\Delta}_{\text{noise}} \sim (R/L)^{t+1}$ and their ratio as $\bar{\Delta}_{\text{signal}}/\bar{\Delta}_{\text{noise}} \sim (L/D)^{t+1}$, see [66] for more details. As a consequence, the signal to noise ratio can be improved by increasing the order of the design t. The precise value of the ratio $\bar{\Delta}_{\text{signal}}/\bar{\Delta}_{\text{noise}}$ will, in general, depend on the chosen orientations $R1$ and $R2$, and the specific form of the signal and noise sources. While signals with smooth spatial variations over the size of the detector should be better decoupled, we would require that the t-design objects are bigger than the wavelength of the probing field, ensuring that the latter is not decoupled, and that the readout of the particle orientation can still take place. As an illustrative example we consider the case of a t-designed object constructed of electric elementary charges distributed at 2 μm distance from the origin at positions determined by the known analytic solutions for t-designs. In practice, these charges could be placed at the tips of neutral cylinders that meet at the center of the sphere and are arranged such that they preserve the symmetry of the t-design, see Fig. 2(a) for the case of $t=2$. The source of the perturbation is taken to be a body of 10^3 elementary charges placed at a distance of $L = 200$ μm. The signal is generated by a single charge placed at a distance of $D = 10$ μm. In Fig. 2(b) we show the scaling of both $\bar{\Delta}_{\text{noise}}$ and $\bar{\Delta}_{\text{signal}}$ with the order to the spherical t-design, which clearly evidences that the sensitivity of the device improves with the order of the t-design.

Following a similar reasoning, one can now consider the possibility of making the source of this signal a second t-designed object, which can also be placed in a superposition of two distinct orientations. The sensitivity to the signal of this source in superposition translates into the capability of generating entanglement between the rotational degrees of freedom of the two objects. More precisely, let us consider that two t-designed objects, A and B, are placed some distance from each other that ensures that their interaction is not negligible, and that they are initially prepared in the product state $(|R1\rangle + |R2\rangle)_A \otimes (|R1\rangle + |R2\rangle)_B$. Then their global state after a time T is given by $(\hbar = 1)$

$$\sum_{i,j} e^{-i(E_{ij}+\Delta_{ij})T} |RiRj\rangle_{AB}, \tag{2}$$

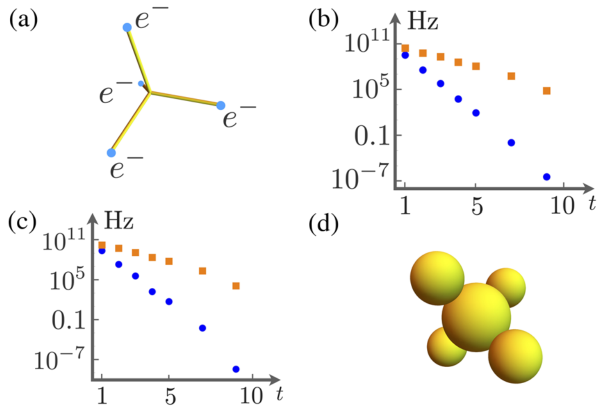

FIG. 2. Numerical analysis. Panel (a) depicts a possible realisation of a 2-design for electric charges. Panel (b) shows the resulting scaling of $\bar{\Delta}_{\text{signal}}$ (orange squares) and $\bar{\Delta}_{\text{noise}}$ (blue dots) as a function of the order of the t-designs. Panel (c) shows the scaling of magnitudes E_{ent} (orange squares) and $\bar{\Delta}_{\text{noise}}$ (blue dots) for two electrically interacting bodies at a distance of 10 μm, each corresponding to a spherical t-design with a radius of 2 μm. In (b) and (c), the noise source is taken to be a body with total charge $10^3 e^-$ at a distance of 200 μm, and rotational states $R1$ and $R2$ are numerically optimized to maximize the signal sensitivity and the entangling rate respectively. Panel (d) depicts a possible realization of a t-design for the generation of gravitationally mediated entanglement.

where E_{ij} is the interaction energy between the bodies when object A is in the rotational state Ri and body B in the rotational state Rj, and $\Delta_{ij} = \Delta_A(Ri) + \Delta_B(Rj)$. The state in Eq. (2) will be entangled if $E_{\text{ent}} = [(E_{11} - E_{12}) + (E_{22} - E_{21})] \neq (2\pi/T)n$ for $n = 0, 1, \ldots$, and if, at the same time, $\bar{\Delta}T \ll 1$ for both solids, so that the relative phase due to the interaction between the two particles is not washed out by the fluctuations of the perturbing field, see [66] for further details. The latter condition can always be ensured by choosing a sufficiently high order in the t-design combined with a sufficiently long duration of the experiment.

We provide a numerical analysis of the scaling of the quantities E_{ent} and $\bar{\Delta}$ with the order of the t-design by simulating the case of two t-designed objects as the one discussed in Fig. 2(b) with their centers placed at a distance of 10 μm. In Fig. 2(c), we show the scaling of both E_{ent} and $\bar{\Delta}$, for t-designs with a known analytic solution to ensure numerical accuracy of the entangling and decoherence rates and find that the perturbing field is suppressed much faster than E_{ent}. This shows that two such bodies can get robustly entangled, suggesting applications of the introduced t-designed objects in quantum technologies.

One could also envision a more ambitious experiment where the entangling force acting on the two t-designed bodies is due to gravity alone. We consider massive solids with the properties of t-designs as the one shown in Fig. 2(d), where a central solid sphere is used to connect several smaller peripheral ones whose centers of mass are placed at the positions determined by specific t-design solutions (in the example a 2-design). Notice that the central sphere does not contribute to energy differences due to rotations, as its mass distribution is unchanged under rotations. For the numerical analysis, we take the case of diamond, with a central sphere of radius 10 μm. We fix the total mass of the object to be 1.83×10^{-11} Kg, and correspondingly adapt the radius of the peripheral spheres for each t-design. We place two such objects at a distance of 200 μm from each other, such that Casimir-Polder forces do not exceed the gravitational interaction, and we assume that the objects are free of spin or charge impurities so that it can be considered that their interaction is dominated by gravity. For such a configuration, we find that $E_{\text{ent}} \sim 16$ Hz for the 1-design, and ~0.1 Hz for a 2-design [see Fig. 2(d)], while the magnitude of the fluctuating phase $\bar{\Delta}$ quickly decays from ~7 Hz for the 1-design to $\sim 10^{-6}$ Hz for the 2-design, when the source of perturbation is taken to be a 100 Kg mass placed 20 m away. The presented results indicate that gravitationally mediated entanglement should be observable in the order of seconds for the first three t-designs, provided that each object can be put in a superposition of two orthogonal rotational states within their coherence time, and that other forms of noise, e.g., scattering of background gas molecules, act in longer timescales, see [66].

Finally, we would like to remark that the spherical t-designs can also find application in designing decoherence-free subspaces for spin degrees of freedom. The key idea is to use the geometry of t-designs to place the spins in space. In particular, consider a set of N spins located at the positions of a specific t-design, all of which are in the state up, $|1\rangle$, and a second set of N spins prepared in state down, $|0\rangle$, located in the positions of the same t-design but rotated with respect to the first set. Given that rotations do not affect the value of the energy up to order t, both sets of spins will see the same energy but with opposite sign, as they are in opposite spin states. It becomes evident that the global spin state $|111, \ldots, 000\rangle$ will not acquire any phase up to the order t of a perturbing magnetic field, and therefore, that the set $\{|111, \ldots, 000\rangle, |000, \ldots, 111\rangle\}$ constitutes a robust basis against magnetic field fluctuations up to order t while maintaining sensitivity to $(t+1)$st order multipole field. This represents a systematic extension of the earlier observation that entanglement can play a beneficial role for metrology in the presence of spatially correlated noise [71,72].

Conclusions.—We have demonstrated that macroscopic superpositions of different orientations of a solid object whose shape is suitably determined following the theory of spherical t-designs can be made robust to decoherence due to perturbing potential fields from external sources to any desired level. Moreover, we argue theoretically and demonstrate numerically that the ratio between phase accumulated from a signal of interest originating from a distance L_{sig} and the rate of decoherence imparted by a field originating from a distance L_{dec} scales as $(L_{\mathrm{dec}}/L_{\mathrm{sig}})^{t+1}$ for $L_{\mathrm{sig}} \ll L_{\mathrm{dec}}$ and can thus be made arbitrarily large. This suggests a route for enhancing the sensing capabilities of levitated particles by the replacement of translational with rotational degrees of freedom [73–76] and offers a plethora of applications in the realm of quantum technologies ranging from sensing to the systematic exploration of rotational degrees of freedom for quantum applications.

We acknowledge support by the ERC Synergy grant BioQ (Grant No. 319130), the EU projects HYPERDIAMOND (Grant No. 667192) and AsteriQs (Grant No. 820394), the QuantERA project NanoSpin, the BMBF project DiaPol, the state of Baden-Württemberg through bwHPC, the German Research Foundation (DFG) through Grant No. INST 40/467-1 FUGG, and the Alexander von Humboldt Foundation through a postdoctoral fellowship.

[1] Y. Wu, F. Jelezko, M. B. Plenio, and T. Weil, Diamond quantum devices in biology, Angew. Chem., Int. Ed. Engl. **55**, 6586 (2016).
[2] A. D. Ludlow, M. M. Boyd, J. Ye, E. Peik, and P. O. Schmidt, Optical atomic clocks, Rev. Mod. Phys. **87**, 637 (2015).
[3] A. D. Cronin, J. Schmiedmayer, and D. E. Pritchard, Optics and interferometry with atoms and molecules, Rev. Mod. Phys. **81**, 1051 (2009).
[4] M. Aspelmeyer, T. J. Kippenberg, and F. Marquardt, Cavity optomechanics, Rev. Mod. Phys. **86**, 1391 (2014).
[5] K. Libbrecht and E. D. Black, Toward quantum-limited position measurements using optically levitated microspheres, Phys. Lett. A **321**, 99 (2004).
[6] L. Viola, E. Knill, and S. Lloyd, Dynamical Decoupling of Open Quantum Systems, Phys. Rev. Lett. **82**, 2417 (1999).
[7] C. A. Ryan, J. S. Hodges, and D. G. Cory, Robust Decoupling Techniques to Extend Quantum Coherence in Diamond, Phys. Rev. Lett. **105**, 200402 (2010).
[8] G. de Lange, Z. H. Wang, D. Ristè, V. V. Dobrovitski, and R. Hanson, Universal Dynamical decoupling of a single solid-state spin from a spin bath, Science **330**, 60 (2010).
[9] B. Naydenov, F. Dolde, L. T. Hall, C. Shin, H. Fedder, L. C. L. Hollenberg, F. Jelezko, and J. Wrachtrup, Dynamical decoupling of a single-electron spin at room temperature, Phys. Rev. B **83**, 081201 (2011).
[10] N. Timoney, I. Baumgart, M. Johanning, A. F. Varon, M. B. Plenio, A. Retzker, and C. Wunderlich, Quantum gates and memory using microwave dressed states, Nature (London) **476**, 185 (2011).
[11] C. Müller, X. Kong, J.-M. Cai, K. Melentijevic, A. Stacey, M. Markham, J. Isoya, S. Pezzagna, J. Meijer, J. Du, M. B. Plenio, B. Naydenov, L. P. McGuinness, and F. Jelezko, Nuclear magnetic resonance spectroscopy with single spin sensitivity, Nat. Commun. **5**, 4703 (2014).
[12] J. Casanova, J. F. Haase, Z.-Y. Wang, and M. B. Plenio, Robust dynamical decoupling sequences for individual spin addressing, Phys. Rev. A **92**, 042304 (2015).
[13] G. M. Palma, K.-A. Suominen, and A. K. Ekert, Quantum computers and dissipation, Proc. R. Soc. A **452**, 567 (1996).
[14] M. B. Plenio, V. Vedral, and P. L. Knight, Quantum error correction in the presence of spontaneous emission, Phys. Rev. A. **55**, 67 (1997).
[15] J. Preskill, Quantum clock synchronization and quantum error correction, arXiv:quant-ph/0010098.
[16] C. Macchiavello, S. F. Huelga, J. I. Cirac, A. K. Ekert, and M. B. Plenio, Decoherence and quantum error correction in frequency standards, in *Quantum Communication, Computing and Measurement* (Kluwer, Dordrecht, 2002), p. 337345.
[17] T. Unden, P. Balasubramanian, D. Louzon, Y. Vinkler, M. B. Plenio, M. Markham, D. Twitchen, I. Lovchinsky, A. O. Sushkov, M. D. Lukin, A. Retzker, B. Naydenov, L. P. McGuinness, and F. Jelezko, Quantum Metrology Enhanced by Repetitive Quantum Error Correction, Phys. Rev. Lett. **116**, 230502 (2016).
[18] R. Demkowicz-Dobrzański, J. Czajkowski, and P. Sekatski, Adaptive Quantum Metrology under General Markovian Noise, Phys. Rev. X **7**, 041009 (2017).
[19] S. Zhou, M. Zhang, J. Preskill, and L. Jiang, Achieving the Heisenberg limit in quantum metrology using quantum error correction, Nat. Commun. **9**, 78 (2018).
[20] D. Layden, S. Zhou, P. Cappellaro, and L. Jiang, Ancilla-Free Quantum Error Correction Codes for Quantum Metrology, Phys. Rev. Lett. **122**, 040502 (2019).
[21] A. Ashkin and J. M. Dziedzic, Optical levitation in high vacuum, Appl. Phys. Lett. **28**, 333 (1976).
[22] A. Ashkin and J. M. Dziedzic, Feedback stabilization of optically levitated particles, Appl. Phys. Lett. **30**, 202 (1977).
[23] T. Li, S. Kheifets, D. Medellin, and M. G. Raizen, Measurement of the instantaneous velocity of a Brownian particle, Science **328**, 1673 (2010).
[24] P. Barker and M. N. Schneider, Cavity cooling of an optically trapped nanoparticle, Phys. Rev. A **81**, 023826 (2010).
[25] D. E. Chang, C. A. Regal, S. B. Papp, D. J. Wilson, J. Ye, O. Painter, H. J. Kimble, and P. Zoller, Cavity opto-mechanics using an optically levitated nanosphere, Proc. Natl. Acad. Sci. U.S.A. **107**, 1005 (2010).
[26] O. Romero-Isart, A. C. Pflanzer, F. Blaser, R. Kaltenbaek, N. Kiesel, M. Aspelmeyer, and J. I. Cirac, Large Quantum Superpositions and Interference of Massive Nanometer-Sized Objects, Phys. Rev. Lett. **107**, 020405 (2011).
[27] T. Li, S. Kheifets, and M. G. Raizen, Millikelvin cooling of an optically trapped microsphere in vacuum, Nat. Phys. **7**, 527 (2011).
[28] U. Delić, M. Reisenbauer, D. Grass, N. Kiesel, V. Vuleti, and M. Aspelmeyer, Cavity Cooling of a Levitated Nanosphere by Coherent Scattering, Phys. Rev. Lett. **122**, 123602 (2019).
[29] U. Delić, M. Reisenbauer, K. Dare, D. Grass, V. Vuletić, N. Kiesel, and M. Aspelmeyer, Motional quantum ground state of a levitated nanoparticle from room temperature, Science **367**, 892 (2020).
[30] J.-F. Hsu, P. Ji, C. W. Lewandowski, and B. DUrso, Cooling the motion of diamond nanocrystals in a magneto-gravitational trap in high vacuum, Sci. Rep. **6**, 30125 (2016).

[31] B. R. Slezak, C. W. Lewandowski, J. F. Hsu, and B. DUrso, Cooling the motion of a silica microsphere in a magneto-gravitational trap in ultra-high vacuum, New J. Phys. **20**, 063028 (2018).

[32] M. Geiselmann, M. Juan, J. Renger, J. M. Say, L. J. Brown, F. J. Garca de Abajo, F. Koppens, and R. Quidant, 3D optical manipulation of a single electron spin, Nat. Nanotechnol. **8**, 175 (2013).

[33] L. P. Neukirch, J. Gieseler, R. Quidant, L. Novotny, and A. N. Vamivakas, Observation of nitrogen vacancy photoluminescence from an optically levitated nanodiamond, Opt. Lett. **38**, 2976 (2013).

[34] R. M. Pettit, L. P. Neukirch, Y. Zhang, and A. N. Vamivakas, Coherent control of a single nitrogen-vacancy center spin in optically levitated nanodiamond, J. Opt. Soc. Am. B **34**, C31 (2017).

[35] M. Scala, M. S. Kim, G. W. Morley, P. F. Barker, and S. Bose, Matter-Wave Interferometry of a Levitated Thermal Nano-Oscillator Induced and Probed by a Spin, Phys. Rev. Lett. **111**, 180403 (2013).

[36] Z.-Q. Yin, T. Li, X. Zhang, and L. M. Duan, Large quantum superpositions of a levitated nanodiamond through spin-optomechanical coupling, Phys. Rev. A **88**, 033614 (2013).

[37] A. Albrecht, A. Retzker, and M. B. Plenio, Testing quantum gravity by nanodiamond interferometry with nitrogen-vacancy centers, Phys. Rev. A **90**, 033834 (2014).

[38] T. M. Hoang, Y. Ma, J. Ahn, J. Bang, F. Robicheaux, Z.-Q. Yin, and T. Li, Torsional Optomechanics of a Levitated Nonspherical Nanoparticle, Phys. Rev. Lett. **117**, 123604 (2016).

[39] T. Delord, L. Nicolas, Y. Chassagneux, and G. Hetet, Strong coupling between a single nitrogen-vacancy spin and the rotational mode of diamonds levitating in an ion trap, Phys. Rev. A **96**, 063810 (2017).

[40] T. Delord, P. Huillery, L. Nicolas, and G. Htet, Spin-cooling of the motion of a trapped diamond, Nature (London) **580**, 56 (2020).

[41] W. Marshall, C. Simon, R. Penrose, and D. Bouwmeester, Towards Quantum Superpositions of a Mirror, Phys. Rev. Lett. **91**, 130401 (2003).

[42] M. Bahrami, M. Paternostro, A. Bassi, and H. Ulbricht, Non-Interferometric Test of Collapse Models in Optomechanical Systems, Phys. Rev. Lett. **112**, 210404 (2014).

[43] O. Romero-Isart, Quantum superposition of massive objects and collapse models, Phys. Rev. A **84**, 052121 (2011).

[44] J. Liu and K.-D. Zhu, Detecting large extra dimensions with optomechanical levitated sensors, Eur. Phys. J. C **79**, 18 (2019).

[45] D. Carney, A. Hook, Z. Liu, J. M. Taylor, and Y. Zhao, Ultralight dark matter detection with mechanical quantum sensors, arXiv:1908.04797.

[46] D. Carney, S. Ghosh, G. Krnjaic, and J. M. Taylor, Gravitational detection of dark matter, arXiv:1903.00492.

[47] C. M. DeWitt and D. Rickles, *The Role of Gravitation in Physics: Report from the 1957 Chapel Hill Conference*, Edition Open Access 2011 (Max Planck Research Library for the History and Development of Knowledge, Berlin, 2011).

[48] D. Kafri, J. M. Taylor, and G. J. Milburn, A classical channel model for gravitational decoherence, New J. Phys. **16**, 065020 (2014).

[49] M. Bahrami, A. Bassi, S. McMillen, M. Paternostro, and H. Ulbricht, Is gravity quantum, arXiv:1507.05733.

[50] M. Carlesso, A. Bassi, M. Paternostro, and H. Ulbricht, Testing the gravitational field generated by a quantum superposition, New J. Phys. **21**, 093052 (2019).

[51] J. Schmöle, M. Dragosits, H. Hepach, and M. Aspelmeyer, A micromechanical proof-of-principle experiment for measuring the gravitational force of milligram masses, Classical Quantum Gravity **33**, 125031 (2016).

[52] S. Bose, A. Mazumdar, G. W. Morley, H. Ulbricht, M. Toroš, M. Paternostro, A. A. Geraci, P. F. Barker, M. S. Kim, and G. Milburn, Spin Entanglement Witness for Quantum Gravity, Phys. Rev. Lett. **119**, 240401 (2017).

[53] T. Krisnanda, G. Y. Tham, M. Paternostro, and T. Paterek, Observable quantum entanglement due to gravity, npj Quantum Inf. **6**, 12 (2020).

[54] J. S. Pedernales, G. W. Morley, and M. B. Plenio, Motional Dynamical Decoupling for Matter-Wave Interferometry, Phys. Rev. Lett. **125**, 023602 (2020).

[55] B. Bajnok, Construction of spherical *t*-designs, Geometriae Dedicata **43**, 167 (1992).

[56] J. Makino, Yet another fast multipole method without multipoles—pseudoparticle multipole method, J. Comput. Phys. **151**, 910 (1999).

[57] A. Bondarenko, D. Radchenko, and M. Viazovska, Optimal asymptotic bounds for spherical designs, Ann. Math. **178**, 443 (2013).

[58] R. N. Hardin and N. J. A. Sloane, McLarens improved snub cube and other new spherical designs in three dimensions, Comput. Geom. **15**, 429 (1996).

[59] R. S. Womersley, Efficient spherical designs with good geometric properties in *Contemporary Computational Mathematics—A Celebration of the 80th Birthday of Ian Sloan*, edited by J. Dick, F. Kuo, and H. Wozniakowski (Spinger, Cham, 2018), pp. 1243–1285.

[60] V. V. Albert, J. P. Covey, and J. Preskill, Robust encoding of a qubit in a molecule, arXiv:1911.00099 [Phys. Rev. X (to be published)].

[61] A. D. Rider, C. P. Blakemore, A. Kawasaki, N. Priel, S. Roy, and G. Gratta, Electrically driven, optically levitated microscopic rotors, Phys. Rev. A **99**, 041802(R) (2019).

[62] J. Millen, T. S. Monteiro, R. Pettit, and A. N. Vamivakas, Optomechanics with levitated particles, Rep. Prog. Phys. **83**, 026401 (2020).

[63] P. Huillery, T. Delord, L. Nicolas, M. Van Den Bossche, M. Perdriat, and G. Htet, Spin mechanics with levitating ferromagnetic particles, Phys. Rev. B **101**, 134415 (2020).

[64] A. Bassi, K. Lochan, S. Satin, T. P. Singh, and H. Ulbricht, Models of wave-function collapse, underlying theories, and experimental tests, Rev. Mod. Phys. **85**, 471 (2013).

[65] M. Carlesso, M. Paternostro, H. Ulbricht, A. Vinante, and A. Bassi, Non-interferometric test of the continuous spontaneous localization model based on rotational optomechanics, New J. Phys. **20**, 083022 (2018).

[66] See the Supplemental Material at http://link.aps.org/supplemental/10.1103/PhysRevLett.125.090501 for a more detailed derivation of the main results and a noise analysis, which includes Refs. [43,47–49,52,63,67–70].

[67] P. Szańkowski, M. Trippenbach, and Y. B. Band, Spin decoherence due to fluctuating fields, Phys. Rev. E **87**, 052112 (2013).

[68] O. Romero-Isart, M. L. Juan, R. Quidant, and J. I. Cirac, Toward quantum superposition of living organisms, New J. Phys. **12**, 033015 (2010).

[69] S. Sellner *et al.*, Improved limit on the directly measured antiproton lifetime, New J. Phys. **19**, 083023 (2017).

[70] L. Martinetz, K. Hornberger, and B. A. Stickler, Gas-induced friction and diffusion of rigid rotors, Phys. Rev. E **97**, 052112 (2018).

[71] U. Dorner, Quantum frequency estimation with trapped ions and atoms, New J. Phys. **14**, 043011 (2012).

[72] J. Jeske, J. H. Cole, and S. F. Huelga, Quantum metrology in the presence of spatially correlated noise: Restoring Heisenberg scaling, New J. Phys. **16**, 073039 (2014).

[73] B. A. Stickler and K. Hornberger, Molecular rotations in matter-wave interferometry, Phys. Rev. A **92**, 023619 (2015).

[74] B. A. Stickler, F. T. Ghahramani, and K. Hornberger, Rotational Alignment Decay and Decoherence of Molecular Superrotors, Phys. Rev. Lett. **121**, 240401 (2018).

[75] B. A. Stickler, B. Papendell, S. Kuhn, B. Schrinski, J. Millen, M. Arndt, and K. Hornberger, Probing macroscopic quantum superpositions with nanorotors, New J. Phys. **20**, 122001 (2018).

[76] M. Carlesso, H. R. Naeij, and A. Bassi, A general approach toward rotational decoherence, arXiv:1912.08159.